IEEE Access
Multidisciplinary | Rapid Review | Open Access Journal

Received January 20, 2021, accepted January 25, 2021, date of publication January 28, 2021, date of current version February 9, 2021.

Digital Object Identifier 10.1109/ACCESS.2021.3055204

An Adaptive Sliding Mode Motion Control Method of Remote Operated Vehicle

ZONGSHENG WANG, YUE LIU, ZHENDONG GUAN, AND YAN ZHANG
College of Ocean Science and Engineering, Shandong University of Science and Technology, Qingdao 266590, China
Corresponding author: Yue Liu (1293817297@qq.com)

ABSTRACT Aiming at the problems of unstable motion and low tracking accuracy caused by complex external disturbance during the movement of the remote operated vehicle(ROV), the adaptive control method and sliding mode control method are combined to propose a ROV adaptive sliding mode motion controller(ASM controller). The sliding mode surface is designed by exponential reaching law and saturation function to achieve rapid convergence of the control system and eliminate high-frequency buffeting, combined with adaptive algorithm to improve the anti-disturbance ability of the system, and the Lyapunov stability criterion is used to verify the controller's stability under uncertain parameters and unknown external disturbances. Simulation experiments show that the designed adaptive sliding mode controller has good maneuverability and tracking performance.

INDEX TERMS ROV, motion control, adaptive, sliding mode control.

I. INTRODUCTION

The marine environment has the complexity and unpredictability, ROV underwater operations are vulnerable to external disturbance, especially are affected by the current impact [1]. The parameters of the ROV motion model are difficult to determine, and its' movement has the characteristics of multivariable, nonlinear and strong coupling. The control system is not stable and its accuracy is not high [2], and when the controller's axial and steering output is allocated to each propeller, the ROV's thrust output is required to be stable to avoid hardware loss caused by high-frequency buffeting [3], [4]. So how to design a motion controller which has the stable and good control performance and tracking performance under the condition of parameter uncertainty and complex external disturbance still has large difficulty.

Sliding mode control is a type of nonlinear control, which can force the system to move according to the state trajectory of a predetermined sliding mode. Because it can overcome the uncertainty of the system, and has excellent performance in fault-tolerant control, it is widely used in ROV motion control, but it's buffeting problem causes thruster loss. In order to solve the nonlinear, unstable and poor tracking performance of ROV, many scholars have done a lot of research work using sliding mode control. Liu *et al.* [5] proposed a new adaptive second-order sliding mode (SOSM) control method combining adaptive strategy and backstepping technique, which was successfully applied to the voltage regulation problem of Buck converter. Ding *et al.* [6] constructed a new state-saturated-like SOSM algorithm, whose advantage lies in that it will provide the maximum domain of attraction under the preset state constraints. Wang *et al.* [7] addressed the investigation of SMC for SPSs with Markov jump parameters. This method avoids the ill-conditioned problems that may occur on the sliding surface and ensure the state trajectories of the system can drive onto the predefined surface globally.

The above studies have respectively solved many problems in ROV sliding motion control and achieved good control effects. However, the problems of buffeting and poor tracking performance are not solved simultaneously. Based on the above studies, this paper proposes an adaptive sliding mode control method to solve the problems of motion instability and low tracking accuracy caused by complex external disturbances of ROV. The α coefficient of traditional sliding mode control cannot guarantee the good robustness of the controller near the sliding mode surface. Moreover, the switching function $sgn(s_i)$ has the characteristics of ultra-high frequency switching, which is easy to cause the high frequency input of the system and thus generate buffeting phenomenon. In addition, when the ROV is continuously disturbed, the controller needs to have stronger anti-interference ability and self-adaptability.

The associate editor coordinating the review of this manuscript and approving it for publication was Hao Shen.

In this paper, an improved exponential approach law is designed to improve the speed of error convergence by using the state error to design the sliding mode surface, and the required control rate function is calculated by combining the second order nonlinear state equation. The buffeting problem is solved by using saturation function $sat(s_i)$ instead of switching function $sgn(s_i)$ so as to avoid power output failure caused by high frequency switching characteristics. In addition, the adaptive law is introduced based on the adaptive algorithm to optimize the performance of the sliding mode controller, so as to realize the dual requirements of ROV control performance and system stability. Finally, the stability of the controller is verified by Lyapunov stability criterion.

II. DESIGN OF A ROV ADAPTIVE SLIDING MODE CONTROLLER (ASM CONTROLLER)

A. ROV MOTION CONTROL SYSTEM

The motion control system of ROV is a nonlinear and uncertain system. Its inputs are the expected positions and attitude angles, and its outputs are the vector torques composed of thrust [8]–[12]. Given the expected path and attitude angle, the controller uses the parameters provided by the navigation system and the characteristics of the ROV itself to calculate the torque required by the actuator on the basis of the model, so that the ROV maintains the posture and navigate along the expected trajectory. The structural block diagram of the ROV's motion control system is shown in Fig. 1.

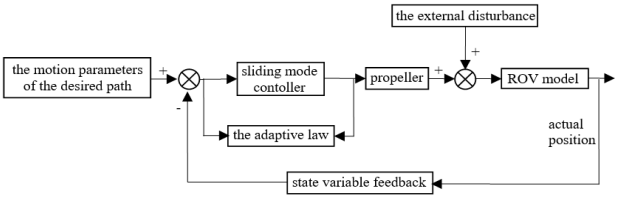

FIGURE 1. ROV motion control system composition.

In this paper, the inertial coordinate system $E\_\xi\eta\zeta$ and motion coordinate system G_xyz are used to describe the posture of ROV, and the coordinate system is established as shown in Fig. 2.

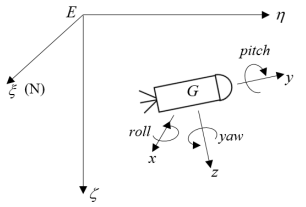

FIGURE 2. ROV's inertial coordinate system and motion coordinate system.

Inertial coordinate system determines the center of the ROV movement, the origin E of the coordinate system fixed on the horizon, the positive zeta-axis is toward the center of the earth, the ksi-axis and the eta-axis unit vectors constitute the right-handed coordinate system, usually the positive ksi-axis is pointing to the north. The motion coordinate system is designed to describe the rotation process of the ROV. The origin G is the center of gravity of the ROV, the positive x-axis is pointing to the ROV's bow, the y-axis is perpendicular to the longitudinal midsection of the hull and points to starboard, and the z-axis is on the longitudinal midsection of the ship and points to the bottom.

ROV's models includes kinematics model and dynamics model [13]–[15]. In this paper, ASM controller is designed based on ROV motion models. Establishing motion models is a necessary process for ROV control system design and simulation analysis.

The kinematics model of ROV describes the parameter expression relationship during the movement and is an abstract representation of the actual physical process. In combination with the free motion characteristics of the general rigid body, the kinematic model of ROV is described as the relationship between the rate of change of position coordinate $\eta_1 = [xyz]^{\mathrm{T}}$ and euler angle coordinate $\eta_2 = [\varphi\theta\psi]^{\mathrm{T}}$ and linear velocity $v_1 = [uvw]^{\mathrm{T}}$ and angular velocity $v_2 = [pqr]^{\mathrm{T}}$. The kinematic model of ROV is established in the above coordinate system as follows:

$$\begin{aligned}
\dot{x} &= u\cos\psi\cos\theta + v(\cos\psi\sin\theta\sin\phi - \sin\psi\cos\phi) \\
&\quad + w(\cos\psi\sin\theta\cos\phi + \sin\psi\sin\phi) \\
\dot{y} &= u\sin\psi\cos\theta + v(\sin\psi\sin\theta\sin\phi - \cos\psi\cos\phi) \\
&\quad + w(\sin\psi\sin\theta\cos\phi + \cos\psi\sin\phi) \\
\dot{z} &= -u\sin\theta + v\cos\theta\sin\phi \\
&\quad + w\cos\theta\cos\phi \\
\dot{\phi} &= p + q\sin\phi\tan\theta + r\cos\phi\tan\theta \\
\dot{\theta} &= q\cos\phi - r\sin\phi \\
\dot{\psi} &= q\sin\phi/\cos\theta + r\cos\phi/\cos\theta
\end{aligned} \tag{1}$$

where:

x, y, z are respectively the position of the ROV relative to the inertial coordinate system. φ, θ, ψ are respectively the euler angle of the ROV relative to the inertial coordinate system. $\dot{x}, \dot{y}, \dot{z}$ are the position change rate of the ROV relative to the inertial coordinate system. $\dot{\varphi}, \dot{\theta}, \dot{\psi}$ are respectively the euler angle change rate of the ROV relative to the inertial coordinate system. u, v, w are respectively the linear velocity of ROV relative to the moving coordinate system. p, q, r are respectively the angular velocity of ROV relative to the moving coordinate system.

The dynamic system of ROV is highly nonlinear, so the motion control of ROV can only be studied by establishing a dynamic model. The ROV is subjected to both hydro-static and hydro-dynamic motion while it moves in water, and the magnitude, direction, and distribution of the reaction force generated by the fluid to the ROV depend on the parameters of the flow force itself. Based on Newton-Euler model, the dynamic model is established as follows:

$$M\dot{v} + C(v)v + D(v)v + g(\eta_2) + \tau_d = \tau \tag{2}$$

where:

M is the inertia matrix of ROV including additional mass.$C(v)$ is the coriolis force matrix and centripetal force

matrix.$D(v)$ is the fluid resistance matrix. $g(\eta_2)$ is the restoring force and torque vector generated by gravity and buoyancy.$\tau \in R^{6\times1}$ is the control input of ROV.$\tau_d \in R^{6\times1}$ is the disturbed current encountered by the ROV.

B. ASM CONTROLLER

In Section II. A, the ROV multi-input multi-output, nonlinear uncertainty model (1)(2) has been established. And the sliding mode control algorithm is adopted in this paper to design the controller. Firstly, the model of ROV controller is defined as the nonlinear standard form shown in Equation (3):

$$\begin{aligned} \dot{x}_1 &= x_2 \\ \dot{x}_2 &= f(x,t) + b(t)\cdot u(t) + d(t) \end{aligned} \tag{3}$$

where:

$x = [x_1, x_2]^{\mathrm{T}} \in R^n$ is the state variable of the system. x_1, x_2 are the state vectors, and their expression are:

$$\begin{aligned} x_1 &= [\eta_1, \eta_2]^{\mathrm{T}} = [x, y, z, \varphi, \theta, \psi]^{\mathrm{T}} \\ x_2 &= [v_1, v_2]^{\mathrm{T}} = [u, v, w, p, q, r]^{\mathrm{T}} \end{aligned} \tag{4}$$

$u(t)$ is the input vector of the controller, and the expre-ssion is:

$$u(t) = [\tau_X, \tau_Y, \tau_Z, \tau_K, \tau_M, \tau_N]^{\mathrm{T}} \tag{5}$$

$f(x,t)$ is a smooth nonlinear function satisfying the requirements of system state variables, and the expression can be obtained according to equation (2):

$$f(x,t) = -\mathrm{M}^{-1}\cdot[(C(x_2) + D(x_2))\cdot x_2 + g(x_1)] \tag{6}$$

$b(t)$ is the control gain function, which satisfies the reversible of the matrix; $d(t)$ is the disturbance function, and the bounded disturbance value is defined.

The design steps of ASM controller are as follows:

Step 1:

Firstly, the sliding surface and its differential function are designed as follows:

$$\begin{aligned} s_i &= \dot{e}_i + \lambda_i \cdot e_i, & \lambda_i > 0 \\ \dot{s}_i &= -K_{1i}\cdot sat(s_i) - R_i \cdot s_i, & R_i \geq 0 \end{aligned} \tag{7}$$

where:

λ_i, R_i are adjustable parameters, $i = 1,2,\cdots,6$.

State error variable is $e_i = x_i - x_{di},\ i = 1,2,\cdots,6$.

$$sat(x) = \begin{cases} \mathrm{sgn}(s_i), & |s_i| > \varepsilon \\ \frac{s_i}{\varepsilon}, & |s_i| \leq \varepsilon \end{cases} \tag{8}$$

$$K_{1i} = \frac{g_i}{h(s_i)} > 0, \quad g_i > 0 \tag{9}$$

The exponential variable $h(x)$ satisfies:

$$\begin{cases} h(s_i) = \gamma_0 + (1-\gamma_0)\cdot e^{-\alpha\cdot|s_i|}, & \alpha > 0, \quad 0 \leq \gamma_0 \leq 1 \end{cases} \tag{10}$$

where:

α represents the parameters of the asymptotic law for an ERL (Exponential Reaching Law) index.γ_0 and g_i are auxiliary adjustable parameters, and they determine the convergence rate and magnitude jointly: with the increase-ment of $|s_i|$, $h(s_i)$ gradually approaches γ_0. Since the convergence rate of $g_i/h(s_i)$ is greater than that of g_i/γ_0, this means that the attraction of the sliding surface is faster. On the other hand, as $|s_i|$ decreases, $h(s_i)$ approaches 1 indefinitely, so $g_i/h(s_i)$ converges to g_i, which forces the system to gradually reduce buffeting as it approaches the sliding surface.

Combined with equations (3) and (7)-(10), the control rate can be obtained:

$$\begin{aligned} u_i(t) = -b(x_i)^{-1}[f(x_i) - \ddot{x}_{di} + \lambda_i\cdot\dot{e}_i \\ + K_{1_i}\cdot sat(s_i) + R_i\cdot s_{i+d_i}] \end{aligned} \tag{11}$$

Step 2:

Since ROV requires high control accuracy and dynamic response, especially when the disturbance continues to change, the controller needs stronger anti-disturbance ability and self-adaptability. Therefore, adaptive algorithm is added to optimize the above sliding mode controller to meet the dual requirements of control performance and system stability.

The error of perturbation estimation is defined as:

$$\tilde{d}_i = d_i - \hat{d}_i \tag{12}$$

where, $\tilde{d}(t)$ is the disturbance estimate error.$\hat{d}(t)$ is the disturbance estimate value.

Assuming that the disturbance function $d(t)$ changes slowly, $\dot{d}(t) = 0$ is considered. The derivative of equation (12) can be obtained as follows:

$$\dot{\tilde{d}}_i = \dot{d}_i - \dot{\hat{d}}_i = -\dot{\hat{d}}_i \tag{13}$$

The control rate can be obtained by substituting the disturbance estimate $\hat{d}(t)$ into equation (11):

$$\begin{aligned} u_i(t) = -b(x_i)^{-1}[f(x_i) - \ddot{x}_{di} + K_{1_i}\cdot sat(s_i) \\ + \hat{d}_i + R_i\cdot s_i + \lambda_i\cdot\dot{e}_i] \end{aligned} \tag{14}$$

In Equation (11), the controller's control rate $u_i(t)$ contains unknown adjustable parameters λ_i, R_i. In Equation (12), the error is defined as $\tilde{d}(t)$, and the goal of the controller is to adjust parameters to minimize the error. The method used in this paper to solve the minimum error is the gradient descent method, which makes the opposite direction of the adjustment parameter change consistent with the negative gradient direction of the error derivative $\dot{\tilde{d}}(t)$ in Equation (13) so as to obtain the minimum value of the error.

The stability of the controller design method with adaptive rate is proved below.

C. PROOF OF STABILITY

To prove the stability of ASM controller designed in the previous section, the following Lyapunov function is constructed:

$$V_i\left(s_i, \tilde{d}_i\right) = \frac{1}{2}s_i^2 + \frac{1}{2\cdot\sigma}\tilde{d}_i^2, \tag{15}$$

where $i = 1,2,\cdots,6$

By differentiating the sliding mode surface (7) of the designed controller, and combining the error formula and the state space equation (3), the following equation can be obtained:

$$\dot{s}_i = f_i + b_i u_i(t) + d_i - \ddot{x}_{di} + \lambda_i \dot{e}_i \tag{16}$$

Further considering the basic requirements of stability, the control rate (14) is combined with equation (15) and equation (16), when $|si| \geq \varepsilon$:

$$\begin{aligned} \frac{dV_i}{dt} &= s_i \cdot \dot{s}_i + \frac{1}{\sigma} \cdot \tilde{d}_i \cdot \dot{\tilde{d}}_i \\ &= \left[-\frac{g_i}{h(s_i)} sat(s_i) - R_i s_i \right] \cdot s_i + \tilde{d}_i \left(s_i - \frac{1}{\sigma} \cdot \dot{\hat{d}}_i \right) \end{aligned} \tag{17}$$

The disturbance estimate $\hat{d}(t)$ satisfies:

$$\dot{\hat{d}}_i = \sigma \cdot s_i = \sigma \cdot (\dot{e}_i + \lambda_i e_i) \tag{18}$$

Combining equations (17) with known constraints such as equation (10) and equation (18), it can be obtained that:

$$\frac{dV_i}{dt} < \left[-\frac{g_i}{\gamma_0} sat(s_i) - R_i \cdot s_i \right] \cdot s_i < \left[\left(-\frac{g_i}{\gamma_0} - R_i \right) \right] \cdot |s_i|^2 \tag{19}$$

Under the constraint of stability conditions, the following equations are always true:

$$-\frac{g_i}{\gamma_0} - R_i < 0 \tag{20}$$

The Lyapunov function constructed in equation (15) satisfies $V_i\left(s_i, \tilde{d}_i\right) > 0$, so it is a positive definite function. It can be seen from equation (19) and equation (20) that its derivative $dV_i/dt < 0$ is a negative definite function, so the constructed function satisfies the asymptotic stability condition of Lyapunov theorem. The stability of the ASM controller is verified.

III. SIMULATION AND VERIFICATION

To verify that the ROV model established has good maneuvering performance and the ASM controller has good tracking performance, the ROV structural parameters studied in this paper are shown in TABLE 1, and the additional mass and hydrodynamic coefficient [16] are shown in TABLE 2:

TABLE 1. ROV structural parameters.

parameter name	symbol	value	unit
mass	m	2500	kg
buoyancy	B	24525	N
gravity	W	24574	N
high buoyancy	Z_B	0.5	m
rotational inertia	I_x	440	kg.m^2
rotational inertia	I_y	1300	kg.m^2
rotational inertia	I_z	1250	kg.m^2
peak output	F_{out}	5000	N

TABLE 2. ROV's additional mass and hydrodynamic coefficient.

parameter	value	parameter	value	parameter	value
X_u	-1636	$\dot{K}_p$	-9810	$X_{u\|u\|}$	-952
Y_v	-2140	$\dot{M}_q$	-19620	$Y_{v\|v\|}$	-1364
Z_w	-3000	$\dot{N}_r$	-7848	$Z_{w\|w\|}$	-3561
$\dot{X}_u$	-3610	K_p	-1664	$K_{p\|p\|}$	-890
$\dot{Y}_v$	-4660	M_q	-1947	$M_{q\|q\|}$	-1876
$\dot{Z}_w$	-11772	N_r	-1524	$N_{r\|r\|}$	-773

A. MANEUVERING PERFORMANCE SIMULATION

The maneuvering performance refers to the ability of ROV to maintain or change the motion state[17]–[20]. The maneuvering performance simulation of ROV is to detect whether there are problems with the motion model and physical parameters without the intervention of a controller. Therefore, simulation was conducted based on the above parameters and on the established ROV motion model in equation (1) and (2).

The control performance of ROV is reflected in the rapid convergence of each axial speed and the fluctuation of each attitude angle when the ROV changes the speed, heading and position. Three-dimensional spiral diving motion is a combination of horizontal motion and vertical motion, which can well reflect the control performance of ROV.In this paper, the three-dimensional spiral diving motion simulation was carried out based on the ROV model in the presence or absence of disturbance. As the peak output value of each ROV propeller is 5000N, the input parameter $u = [1000, 1000, 0, 0, 0, 100]^{\mathrm{T}}$ is selected. The disturbance model selects the three-axis axial interference force. At this time, the ROV's motion does not have controller intervention, and the amplitude of any given three-axis axial interference force is 100N. The simulation results were shown in Fig. 3:

It can be seen that the ROV trajectory accords with spiral diving trajectory from the motion projection and three-dimensional trajectory of each plane in Fig. 3(a). As can be seen from Fig. 3(b), each axial movement speed of ROV can converge rapidly when it makes a spiral dive in three-dimensional space in a non-disturbance environment. The lateral component velocity stability in the 0.7 m/s, longitudinal component velocity stability in the 0.6 m/s, vertical component velocity stability in the 0.2 m/s. As can be seen from the three posture angular velocities, the lateral and longitudinal angular velocities fluctuate in a small amplitude

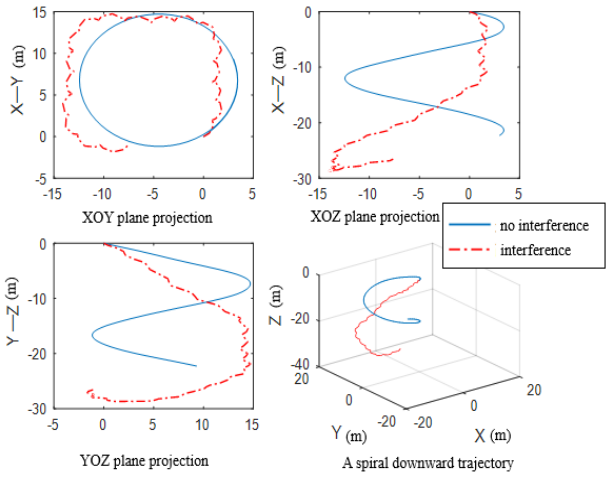

(a) ROV's inertial coordinate system and motion coordinate system

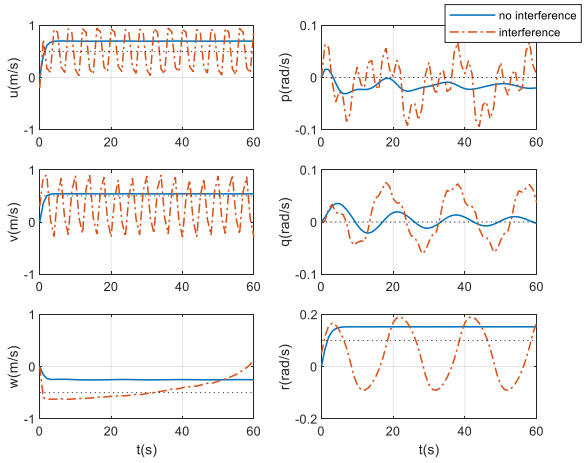

(b) ROV three-dimensional spiral dive Linear velocity and angular velocity

FIGURE 3. ROV Maneuverability simulation.

near 0, and the bow roll angular velocity finally stability in the 0.11 rad/s. Therefore, the motion model and physical parameters of ROV ensure its good handling performance.

As can be seen from Fig. 3, the ROV loses control of its motion after disturbance is added.

B. TRACKING PERFORMANCE SIMULATION

Tracking performance refers to the ROV's ability to follow the expected trajectory, and reflect in the size of the three-dimensional path tracking position error. As can be seen from Fig.3, after adding the external disturbance, the ROV's motion trajectory deviated seriously from the expected trajectory. Therefore, the controller is introduced to solve ROV's poor tracking performance and low tracking accuracy which are caused by external disturbance.

Compared with the traditional sliding mode controller, the simulation is performed under the expected excitation and disturbance intervention to verify whether the designed ASM controller in this paper can guarantee the good tracking performance of ROV.

Take the three-dimensional spiral diving path as the expected value, and take (-5, 5) as the center of the circle for the spiral diving. If the ROV angle speed is set to be too high, the diving depth will be reduced and the diving track graph may overlap and be difficult to recognize. Therefore, the ROV angle speed is set as $\omega = 0.05\pi$ and the expected path is set as follows:

The expected position $\eta_{1d}\,(x_d, y_d, z_d)$ is:

$$\begin{aligned} x_d &= c(0.05\cdot\pi\cdot t)\cdot\sqrt{25+10\,(s(0.05\cdot\pi\cdot t)-c(0.05\cdot\pi\cdot t))} \\ y_d &= s(0.05\cdot\pi\cdot t)\cdot\sqrt{25+10\,(s(0.05\cdot\pi\cdot t)-c(0.05\cdot\pi\cdot t))} \\ z_d &= -0.25\cdot t \end{aligned} \tag{21}$$

The expected attitude $\eta_{2d}\,(\phi_d, \theta_d, \psi_d)$ is:

$$\begin{aligned} \phi_d &= 0 \\ \theta_d &= 0 \\ \psi_d &= 0.05\cdot\pi\cdot t \end{aligned} \tag{22}$$

Trigonometric functions are used to simulate the time-varying characteristics of ocean current disturbances. The current velocity U_c and the current velocity angle γ in the disturbance model are defined as follows:

$$\begin{aligned} U_c &= 0.15\cdot s(0.2\cdot\pi\cdot t)+0.05\cdot rand \\ \gamma &= 10\cdot s(0.2\cdot\pi\cdot t)+2\cdot rand \end{aligned} \tag{23}$$

The three groups of small, medium and large disturbance forces were applied to the ROV, and the angular velocity was set to be twice that of the ROV.

1) The small external disturbance force are:

$$\begin{aligned} \Delta f_x &= 400\cdot s(0.1\cdot\pi\cdot t)+20\cdot rand \\ \Delta f_y &= 400\cdot c(0.1\cdot\pi\cdot t)+20\cdot rand \\ \Delta f_z &= 400\cdot s(0.1\cdot\pi\cdot t)+20\cdot rand \end{aligned} \tag{24}$$

2) The medium external disturbance force are:

$$\begin{aligned} \Delta f_x &= 800\cdot s(0.1\cdot\pi\cdot t)+20\cdot rand \\ \Delta f_y &= 800\cdot c(0.1\cdot\pi\cdot t)+20\cdot rand \\ \Delta f_z &= 800\cdot s(0.1\cdot\pi\cdot t)+20\cdot rand \end{aligned} \tag{25}$$

3) The large external disturbance force are:

$$\begin{aligned} \Delta f_x &= 1200\cdot s(0.1\cdot\pi\cdot t)+20\cdot rand \\ \Delta f_y &= 1200\cdot c(0.1\cdot\pi\cdot t)+20\cdot rand \\ \Delta f_z &= 1200\cdot s(0.1\cdot\pi\cdot t)+20\cdot rand \end{aligned} \tag{26}$$

where: $s = \sin$, $c = \cos$, f_x, f_y, f_z are the external disturbance forces exerted on ROV in the directions of x-axis, y-axis, and z-axis respectively. And rand is a normally distributed random item.

Input parameters of controller are shown in TABLE 3:

The ROV's continuous diving depth is set as 20m, and the plane motion trajectory is elliptic trajectory. According to the established simulation environment and controller input,

TABLE 3. Parameters of controller.

parameter	value
K_{1i}	diag(1350,1300,2400,10,10,135)
R_i	diag(2,2,2,1,1,2)
λ_i	diag(250,250,275,0,0,200)
α	2
γ_0	0.1

simulation is carried out under the expected path excitation. The expected time is set as T=30s. The motion trajectory and each plane projection are shown in Fig. 4.

It can be seen from Fig. 4 that, under the perturbation condition, the ROV's motion trajectory has no obvious loss of control after introducing the traditional sliding mode controller and the ASM controller in this paper. It can be seen from Fig. 4(a), (b) and (c) that the motion trajectory of ASM controller under different disturbance forces is closer to the expected trajectory than that of the traditional sliding mode controller, which significantly improves the tracking accuracy. By comparing Fig. 4(a) and Fig. 4(b), it can be seen that ROV shows good tracking accuracy when the disturbance force is the small force 400N and the medium force 800N, and the tracking accuracy of the latter is slightly lower than that of the former. It can be seen from Fig. 4(c) that the tracking effect is poor when the large disturbance force is 1200N.

To further verify the tracking performance of ASM controller, the relative error of each axial three-dimensional path tracking position of the traditional sliding mode controller and ASM controller is shown in Fig.5.

In Fig. 5, Xe,Ye and Ze are the position relative errors in the transverse, longitudinal and vertical directions respectively. According to the position error shown in Fig. 5, the traditional sliding mode controller has a large error when subjected to continuous disturbance, and ASM controller significantly reduces the position error of each axis.

It can be seen from Fig. 5(a) and Fig. 5(b) that under the condition of applying the small disturbance force 400N to ROV, the position relative error of x-axis is within the range of $\pm$ 8%, the relative error of y-axis is within the range of $\pm$ 6% and the relative error of z-axis is within the range of $\pm$ 4% of the traditional sliding mode controller. Each axial position relative error does not converge and has the tendency of infinite fluctuation. After the disturbance force was increased by 100% to 800N, the error range of each axis position remained basically unchanged but the fluctuation frequency increased significantly. The axial relative error of ASM controller, especially the z-axis position relative error, decreases significantly. After T=30s, the relative error of each axis position converges to $\pm$ 2% rapidly, which proves

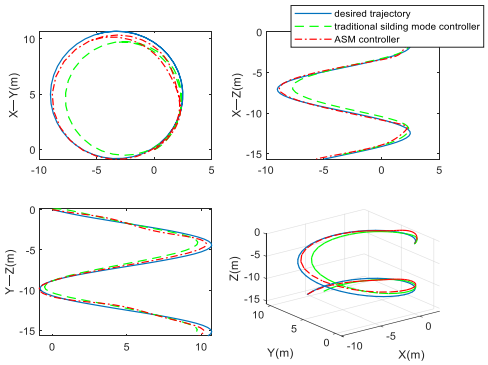

(a) when f = 400N ROV motion trajectory and plane projection

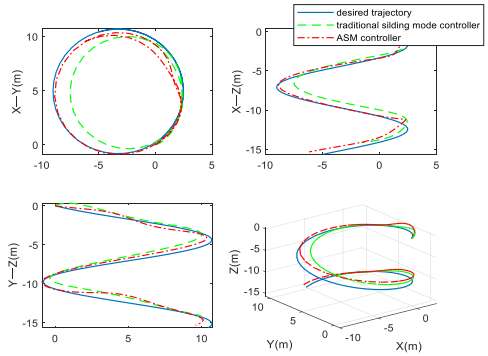

(b) when f = 800N ROV motion trajectory and plane projection

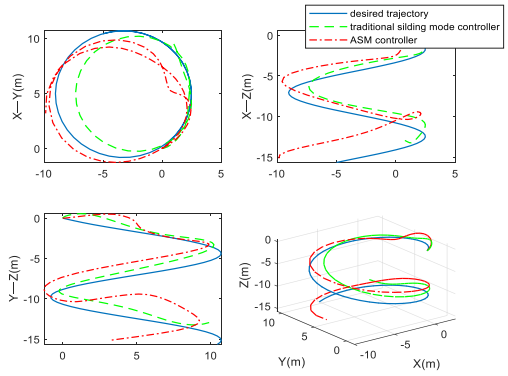

(c) when f = 1200N ROV motion trajectory and plane projection

FIGURE 4. ROV three-dimensional path tracking motion trajectory and plane projection.

that ASM controller can reduce the position error and converge rapidly.

According to Fig. 5(c), under the large disturbance force of 1200N, the axial errors of ASM controller increase and the convergence effect is poor.

In Fig. 6, the output thrust of the eight thrusters of the traditional sliding mode controller and the ASM controller are compared. The traditional sliding mode controller has obvious buffeting phenomenon and the output thrust is unstable. As shown in Fig. 6(a) and Fig. 6(b), when the disturbance force is the small force 400N and the medium force 800N, the ASM controller realizes the stable thrust output of the propeller, and the output is limited to the power peak value of 5000N. The output curve is smooth, which solves

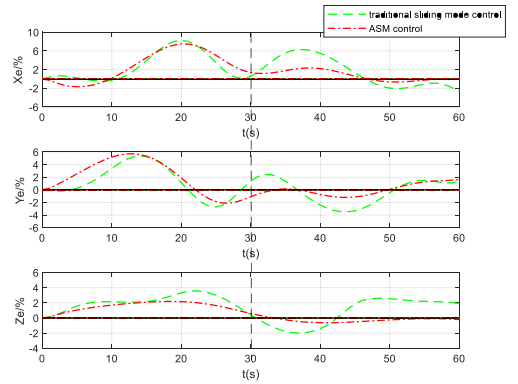

(a) when f = 400N each axial tracking position error

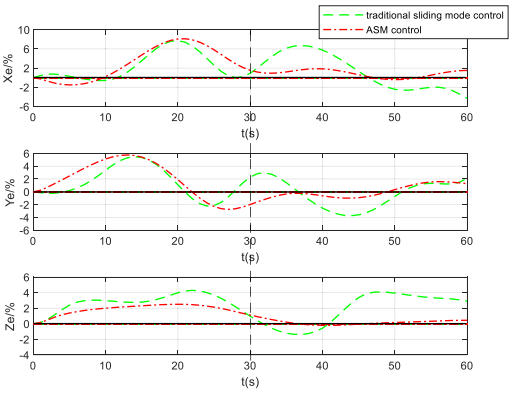

(b)when f = 800N each axial tracking position error

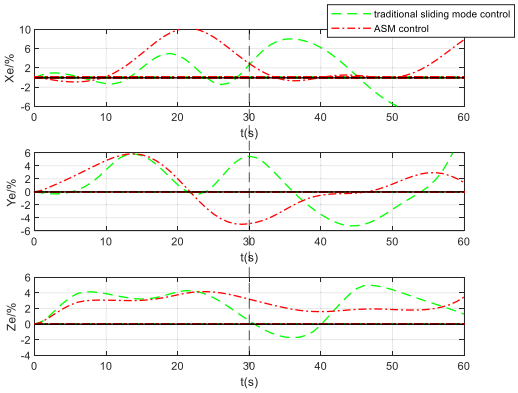

(c) when f = 1200N each axial tracking position error

FIGURE 5. **ROV three-dimensional path tracking position relative error.**

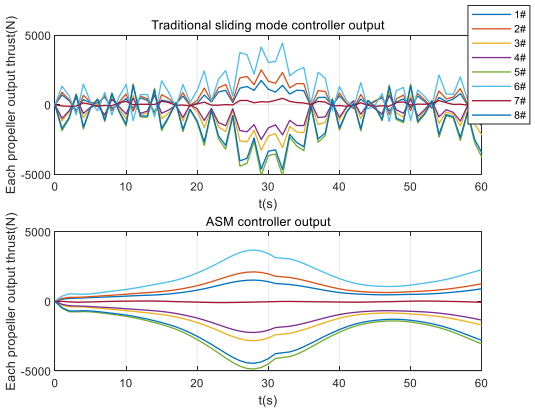

(a)when f = 400N output thrust

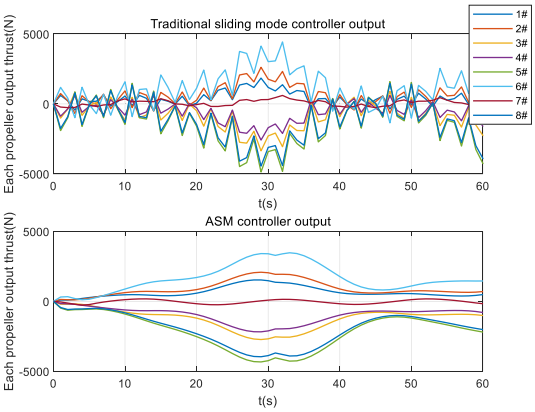

(b) when f = 800N output thrust

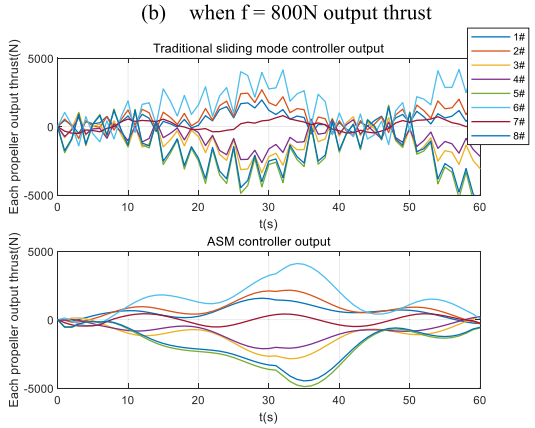

(c)when f = 1200N output thrust

FIGURE 6. **Comparison of output curve stability between traditional sliding mode controller and adaptive sliding mode controller.**

the buffeting problem and avoids the loss of the propeller. It can be seen from Fig. 6(c) that when the disturbance force increases to 1200N, the output thrust curve is not smooth and its stability is poor.

It can be seen from Fig. 4, Fig. 5 and Fig. 6 that, compared with the traditional sliding mode controller, the motion trajectory of ASM controller is closer to the expected trajectory, the axial position error of each controller is significantly reduced, and rapid convergence is achieved within the expected time, and the output thrust is stable. The tracking performance of ASM controller is good when the ROV is applied with disturbance force of 400N and 800N, but the performance is reduced under the disturbance force of 1200N and the desired effect is not achieved.

IV. CONCLUSION

Aiming at the problem of unstable motion and low tracking accuracy caused by complex external disturbance during ROV movement, the following contents are completed in this paper:

(1) Based on the motion model, an adaptive sliding mode controller (ASM controller) is designed. This controller has the following advantages: 1) The tracking position error is

reduced and fast convergence is realized, which solves the problem of infinite convergence time of traditional sliding mode controller; 2) The power output curve is smooth, which solves the buffeting problem; 3) Adaptive control is added to improve the anti-disturbance ability of the controller.

(2) Simulation verifies the ROV model has good manoeuvrability. And verify the ROV control system within the disturbing force of 1000N under the condition of three-dimensional spiral dive path tracking. The traditional sliding mode control error is large, and the adaptive sliding mode control algorithm is advanced, high tracking precision. All the axial errors are obviously reduced and can converge rapidly, and the propeller smooth power output, export thrust within 5000N which realize the position of ROV movement, posture has good control effect.

This paper also needs to be improved in the following two aspects:

(1) ASM controller is a full state feedback control. Since the disturbance is uncertain and the controller still has a certain hysteresis, it can be considered to increase the observer to estimate the disturbance.

(2) When ROV is controlled, control requirements such as optimal path and obstacle avoidance planning are not taken into account, which should be considered in the subsequent work.

REFERENCES

[1] G. Zhenhui and S. Xianpeng, "Deep sea technology and sustainable development," *Ocean Develop. Manage.*, vol. 28, no. 07, pp. 41–46, 2011.
[2] C. J. Fallaha, M. Saad, H. Y. Kanaan, and K. Al-Haddad, "Sliding-mode robot control with exponential reaching law," *IEEE Trans. Ind. Electron.*, vol. 58, no. 2, pp. 600–610, Feb. 2011.
[3] L. Crowder and E. Norse, "Essential ecological insights for marine ecosystem-based management and marine spatial planning," *Mar. Policy*, vol. 32, no. 5, pp. 772–778, Sep. 2008.
[4] R. D. Christ and R. L. Wernli, "The ROV manual, second edition: A user guide for remotely operated vehicles," *Ocean News Technol.*, vol. 20, no. 1, p. 656, 2014.
[5] L. Liu, W. X. Zheng, and S. Ding, "An adaptive SOSM controller design by using a Sliding-Mode-Based filter and its application to buck converter," *IEEE Trans. Circuits Syst. I, Reg. Papers*, vol. 67, no. 7, pp. 2409–2418, Jul. 2020.
[6] S. Ding, K. Mei, and S. Li, "A new second-order sliding mode and its application to nonlinear constrained systems," *IEEE Trans. Autom. Control*, vol. 64, no. 6, pp. 2545–2552, Jun. 2019.
[7] J. Wang, C. Yang, H. Shen, J. Cao, and L. Rutkowski, "Sliding-mode control for slow-sampling singularly perturbed systems subject to Markov jump parameters," *IEEE Trans. Syst., Man, Cybern. Syst.*, early access, Mar. 24, 2020, doi: 10.1109/TSMC.2020.2979860.
[8] O. Elhaki and K. Shojaei, "Neural network-based target tracking control of underactuated autonomous underwater vehicles with a prescribed performance," *Ocean Eng.*, vol. 167, pp. 239–256, Nov. 2018.
[9] F. Rezazadegan, K. Shojaei, F. Sheikholeslam, and A. Chatraei, "A novel approach to 6-DOF adaptive trajectory tracking control of an AUV in the presence of parameter uncertainties," *Ocean Eng.*, vol. 107, pp. 246–258, Oct. 2015.
[10] A. B. Farjadian, M. J. Yazdanpanah, and B. Shafai, "Application of reinforcement learning in sliding mode control for buffeting reduction," in *Proc. World Congr. Eng. Comput. Sci.*, 2013, pp. 53–59.
[11] F. Repoulias and E. Papadopoulos, "Planar trajectory planning and tracking control design for underactuated AUVs," *Ocean Eng.*, vol. 34, nos. 11–12, pp. 1650–1667, Aug. 2007.
[12] C. Chin and M. Lau, "Modeling and testing of hydrodynamic damping model for a complex-shaped remotely-operated vehicle for control," *J. Mar. Sci. Appl.*, vol. 11, no. 2, pp. 150–163, Jun. 2012.
[13] B. Subudhi and D. Jena, "A differential evolution based neural network approach to nonlinear system identification," *Appl. Soft Comput.*, vol. 11, no. 1, pp. 861–871, Jan. 2011.
[14] Z. Bochao and H. Liying, *Sliding Mode Variable Structure Control-Quantitative Feedback Control Method*. Beijing, China: Science Press, 2016, pp. 25–29.
[15] L. Messikh, E. H. Guechi, and M. L. Benloucif, "Critically damped stabilization of inverted-pendulum systems using continuous-time cascade linear model predictive control," *J. Franklin Inst.*, vol. 354, no. 16, pp. 7241–7265, Nov. 2017.
[16] J. Yao, *Theoretical Basis of Ship Maneuverability*. Wuhan, China: Wuhan Univ. of Technolgy Press, 2018, pp. 14–15.
[17] Z. H. Ismail and M. W. Dunnigan, "A region boundary-based control scheme for an autonomous underwater vehicle," *Ocean Eng.*, vol. 38, nos. 17–18, pp. 2270–2280, Dec. 2011.
[18] L. McCue, "Handbook of marine craft hydrodynamics and motion control [bookshelf]," *IEEE Control Syst. Mag.*, vol. 36, no. 1, pp. 78–79, Feb. 2016.
[19] Z. Yan, M. Wang, and J. Xu, "Robust adaptive sliding mode control of underactuated autonomous underwater vehicles with uncertain dynamics," *Ocean Eng.*, vol. 173, pp. 802–809, Feb. 2019.
[20] M. Roopaei, B. Sahraei, and T.-C. Lin, "Adaptive sliding mode control in a novel class of chaotic systems," *Commun. Nonlinear Sci. Numer. Simul.*, vol. 15, no. 12, pp. 4158–4170. Dec. 2010.

ZONGSHENG WANG was born in Zibo, Shandong, China, in 1976. He received the Ph.D. degree. He has taught at the Shandong University of Science and Technology, since 2000, where he is currently a Master Tutor. He is involved in teaching and scientific research on signal detection technology and automatic control systems. His research interests include signal detection, source locating technology, and magnetic bearing control systems.

YUE LIU was born in Dezhou, Shandong, China, in 1997. She received the bachelor's degree in measurement and control technology and instrumentation from the Shandong University of Science and Technology, in 2018, where she is currently pursuing the master's degree in the field of testing and measurement technology and instruments.

ZHENDONG GUAN was born in Zibo, Shandong, China, in 1992. He received the bachelor's degree in measurement and control technology and instrumentation and the master's degree in testing and measurement technology and instruments from the Shandong University of Science and Technology, in 2017 and 2020, respectively.

YAN ZHANG was born in Hengshui, Hebei, China, in 1994. She received the bachelor's degree in electronic information engineering from the Shandong University of Science and Technology, in 2016, where she is currently pursuing the master's degree in the field of testing and measurement technology and instruments.